Applications of phasor plots to in vitro protein studies

Nicholas G. James [a], Justin A. Ross [a], Martin Štefl [b], David M. Jameson [a,*]

[a] Department of Cell and Molecular Biology, John A. Burns School of Medicine, University of Hawaii, Honolulu, HI 96813, USA
[b] J. Heyrovský Institute of Physical Chemistry, v.v.i., Academy of Sciences of the Czech Republic, Dolejškova 3, Prague 18223, Czech Republic

ARTICLE INFO

ABSTRACT

In a recent article, we described the application of phasor analysis to fluorescence intensity decay data on in vitro samples. As detailed in that article, this method provides researchers with a simple graphical method for viewing lifetime data that can be used to quantify individual components of a mixture as well as to identify excited state reactions. In the current article, we extend the use of in vitro phasor analysis to intrinsic protein fluorescence. We show how alterations in the excited state properties of tryptophan residues are easily visualized using the phasor method. Specifically, we demonstrate that protein–ligand and protein–protein interactions can result in unique shifts in the location of phasor points, indicative of protein conformational changes. Application of the method to a rapid kinetic experiment is also shown. Finally, we show that the unfolding of lysozyme with either urea or guanidine hydrochloride results in different phasor trajectories, indicative of unique denaturation pathways.

© 2010 Elsevier Inc. All rights reserved.

Excited state fluorescence lifetime measurements have become a popular and powerful method for gaining information on the local environment of fluorophores in biomolecular systems such as proteins, membranes, and nucleic acids. Excited state intensity decay (lifetime) data are typically obtained using either time domain or frequency domain methods [1,2]. In time domain measurements, the sample is excited with a short pulse of light and the time evolution of the fluorescence intensity decay is recorded, whereas in frequency domain measurements, the sample is typically (but not always) excited with sinusoidally modulated light and the shift in phase and modulation of the emission with respect to the excitation is recorded. Data from each method are essentially equivalent, with the frequency domain data being the Fourier transform of the time domain data [3]. Traditional methods of extracting decay parameters involve fitting the data to models, such as discrete exponentials or distributions [4], until a "good" fit, as judged by the χ^2 value, is reached. A model-less approach, the maximum entropy method, has also been used to describe excited state decay data in terms of the intensity decay components [5]. For a large number of seemingly simple fluorophore systems (e.g., proteins containing a single tryptophan residue), however, the excited state decay cannot be described by single- or even multiexponential models. In some cases, the complexities of the decay may be due to the fact that the fluorophore can sample different molecular environments during the excited state lifetime or to the presence of excited state reactions such as resonance energy transfer, dipolar relaxation, and transient quenching mechanisms.

Tryptophan residues are the most commonly used intrinsic protein probes, and their popularity increased when the method of site-directed mutagenesis allowed the removal or insertion of these residues into specific locations in the protein sequence (although we note that tyrosine fluorescence has also been used in the case of proteins lacking tryptophan residues). The sensitivity of tryptophan's fluorescence properties, including its emission maximum, quantum yield, and lifetime, to local environments in the protein matrix has been used by a number of researchers over the years to characterize a variety of biological processes [2,6–8]. The use of tryptophan analogs, introduced into proteins using molecular biological methods, has also become increasingly popular in studies of protein fluorescence [9,10]. A complete description of all such applications to protein systems is beyond the scope of this article, however, a few examples include the use of tryptophan fluorescence to monitor ligand interactions [11,12], kinetic rate determinations [13,14], and protein–protein, protein–DNA, and protein–RNA interactions [15,16] as well as structural and dynamic features of proteins [17–19] and Förster resonance energy transfer (FRET)[1] [20]. Excited state characterization of tryptophan, free in

---

[1] Abbreviations used: FRET, Förster resonance energy transfer; NATA, N-acetyl-L-tryptophanamide; HSA, human serum albumin; $Na_2S_2O_3$, sodium thiolsulfate; GdHCl, guanidine hydrochloride; PH, pleckstrin homology; GED, GTPase effector region; PRD, proline/arginine-rich domain; hTF, human serum transferrin; hTF N-lobe, recombinant N-lobe of human serum transferrin comprising residues 1–337; FLIM, fluorescence lifetime imaging.

solution and incorporated into proteins, has revealed the complex decay parameters for this intrinsic probe [21]. The environmental sensitivity of tryptophan's ^1L_A transition [22], the possibility of tryptophan rotamer conformations within the protein matrix [23], and excited state reactions of tryptophan residues with neighboring amino acid side chains [24] all have been suggested to play a role in the nonexponential behavior of tryptophan decay [2].

Analyzing tryptophan lifetimes using the traditional approaches, including fits to discrete exponentials or continuous distributions, does not always allow an adequate description of the decay process or provide meaningful physical interpretation. In addition, many proteins have multiple tryptophan residues and may exhibit energy transfer between these residues, and this frustrates attempts to fit the lifetime data to straightforward models. In many cases, however, the goal is simply to use the intrinsic protein fluorescence to monitor a process such as ligand binding, unfolding, or refolding or to detect a conformational change in a particular region of the protein. In such cases, a less constrained approach may provide a useful tool for monitoring alterations in intrinsic protein decay. The phasor plot offers such an approach, although we note that quantitative information can also be obtained.

We recently explored the application of the phasor approach to in vitro studies and briefly described its general utility in the characterization of heterogeneous emissions and systems demonstrating dipolar relaxation as well as intrinsic protein fluorescence [25]. In the previous article, we discussed the basics of the phasor approach and illustrated its application to heterogeneous mixtures of fluorophores as well as excited state reactions such as dipolar relaxation and FRET. In the current article, we extend these observations to studies of protein conformations. Specifically, we apply the phasor plot approach to a number of protein-related systems, including the effect of pH on tryptophan's lifetime, quenching, and the effect of ligand binding, kinetics, protein–protein interactions, and protein unfolding pathways.

Materials and methods

L-Tryptophan and Mes were obtained from Fluka (St. Louis, MO, USA). N-Acetyl-L-tryptophanamide (NATA), fluorescein, human serum albumin (HSA), KI, NaCl, sodium thiolsulfate ($Na_2S_2O_3$), ethanol, Ches, and Hepes were obtained from Sigma (St. Louis, MO, USA). Lysozyme was obtained from Fisher Scientific (Pittsburgh, PA, USA). Thrombin (alpha) and antithrombin III were purchased from Hematologic Technologies (Essex Junction, VT, USA). Sephacryl S-300 resin was obtained from GE Healthcare (Piscataway, NJ, USA). Guanidine hydrochloride (GdHCl) was obtained from Mann Research Laboratories. Urea was purchased from ICN Biomedicals (Irvine, CA, USA). Dynamin 2 was a generous gift from Joseph Albanesi and Barbara Barylko (University of Texas Southwestern Medical School). Recombinant human serum transferrin N-lobe, residues 1–337, was a generous gift from Anne B. Mason (University of Vermont).

HSA purification

Many reports have detailed the fact that even 99% pure lyophilized HSA contains up to 10% higher order oligomers such as dimers, trimers, tetramers, and higher order aggregates formed via disulfides linkage (see, e.g., [26]). To isolate the monomeric protein, HSA (20 mg/ml) was loaded onto a 100-ml Sephacryl S-300 column equilibrated with 20 mM Hepes (pH 7.5). Identification of the oligomeric state and purity of each fraction were determined by nondenaturing native gel electrophoresis (data not shown). The final half of the dominant (monomeric) peak was pooled. HSA concentration was determined using 34,445 $M^{-1}\,cm^{-1}$ as the molar absorption coefficient at 280 nm [27].

Time-resolved measurements

Phase and modulation data were obtained with an ISS Chronos Fluorometer using either a 280- or 300-nm LED as the light source [28]. The bandpass filter FF01-280/20-25 or FF01-295/15-25 (Semrock, Rochester, NY, USA) was used where appropriate, with the excitation light and the emission collected through a longpass filter (WG315 or WG320, Schott) or a 357/50-nm bandpass filter. Polarizers were set at magic angles to eliminate polarization effects [29]. Reference lifetime standard of NATA at pH 7.5 (2.70 ns at 25 °C and 2.95 ns at 20 °C) was used at an excitation wavelength of 280 or 300 nm [30]. For those experiments in which temperature was varied, glycogen (0.00 ns) was used as a reference. Absorbance values at the exciting wavelengths were kept below 0.05 to avoid inner filter affects.

For measurements involving acrylamide quenching, small aliquots of an 8-M stock solution were added to the sample cuvette to obtain the desired acrylamide concentration. For KI quenching, NaCl was present to maintain the ionic strength between each measurement. The stock solution of KI (3 M) contained a small amount (10^{-4} M) of $Na_2S_2O_3$ to prevent the formation of I_3^-, which absorbs in the excitation region of tryptophan fluorescence.

Phasor plots

The theory underlying the phasor approach is presented in another article [31].

Results and discussion

Tryptophan lifetime/phasor as a function of pH

The sensitivity of tryptophan fluorescence to a number of factors (pH, temperature, and polarity of solvent/environment) makes it ideal to monitor alterations in the protein matrix. Such sensitivity has also made interpretation of fluorescence changes in response to specific biological events difficult at best, highlighting the complexity of this fluorescent probe. We examined the excited state properties of L-tryptophan under changing conditions to illustrate the application of the phasor method for analyzing the heterogeneous lifetime decay of proteins. The phasor plot for L-tryptophan as a function of pH (at 25 MHz) is shown in Fig. 1. As the pH is increased from 6.0 to 11.0, the zwitterion form of tryptophan is converted to the anion form ($pK_a \sim 9.39$), each of these forms has its own unique lifetime and quantum yield [2,32–34]. At pH 9.5, there should be a nearly 1:1 anion-to-zwitterion molecular ratio. However, we should note that the phasor point corresponding to pH 9.5 is not midway between the high and low pH points. The exact distance of the phasor point along the line joining the starting and ending points on the universal circle depends not only on the relative concentration but also on the quantum yields of the species in question (in the case of L-tryptophan, the ratio of the lifetimes and quantum yields of the anion-to-zwitterion forms is ~2.8 [34]). The frequencies used will also weight the fractional contributions of the components differently, that is, lower frequency phasor points will weight the longer lifetime component, whereas higher frequencies will favor the shorter component [35].

Quenching and temperature studies

Quenching of a protein's intrinsic tryptophan fluorescence, with molecules such as I^-, NO_3^-, Cs^-, acrylamide, and molecular oxygen [17–19], is commonly used to probe the dynamics of protein matrices. Chemical quenchers may provide information on the exposure of a tryptophan residue to the solvent as a consequence
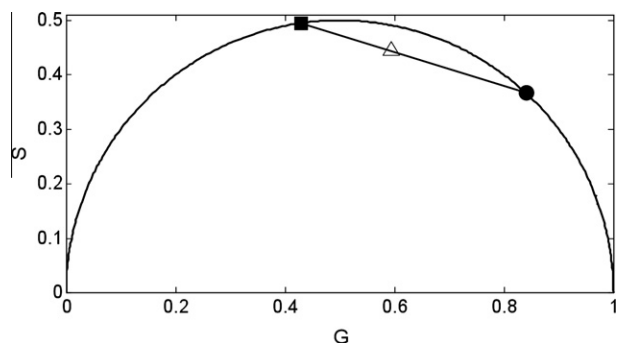
Fig.1. Phasor plot of ʟ-tryptophan at various pH values. The points represent pH 6.0 (circle), pH 9.5 (triangle), and pH 11.0 (square) data at 25 MHz. The lifetime data were collected at 280 nm excitation and 25 °C.

of collision of the excited fluorophore with the quencher molecule (dynamic quenching) or, in some cases, by formation of a ground state dark complex (static quenching) [1]. Both steady state and time-resolved methodologies can be used to obtain quenching information.

As shown in Fig. 2, we examined the effects of quenching molecules on the phasor plot of tryptophan-containing samples. NATA was chosen as a model system because it has a single-exponential decay under our conditions, and the quenching with acrylamide is expected to move the phasor toward shorter lifetimes along the universal circle. The protein lysozyme was used because the photophysics of the tryptophans in this protein have been well investigated [36,37]. Fig. 2 shows the quenching of NATA and lysozyme using the quencher acrylamide. The data were recorded at 89 MHz and 20 °C using a 300-nm LED as the excitation source, and emission was observed through a WG315 longpass filter. As expected, the position of the phasor points is dependent on the quencher concentration. The lifetime of NATA is a single exponential at each quencher concentration and follows a clockwise trajectory along the universal circle toward $G = 1.0$ and $S = 0$ (i.e., 0 ns). With lysozyme, one notes that the phasor points are all within the universal circle, indicating the heterogeneous nature of the lifetime data. The addition of acrylamide results in shorter lifetimes, indicating that one or more of the tryptophan residues in lysozyme are sensitive to dynamic quenching, and the subsequent shift in the phasor points in a clockwise direction. The addition of the quencher iodide (data not shown) also shifted the phasor point, following a similar trajectory to shorter lifetimes, albeit to a lesser extent, as with the acrylamide quenching.

Temperature studies are often used to study protein stability and dynamic aspects of the protein matrix [38]. We examined
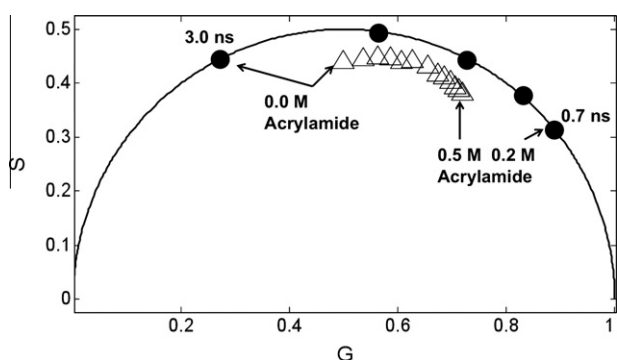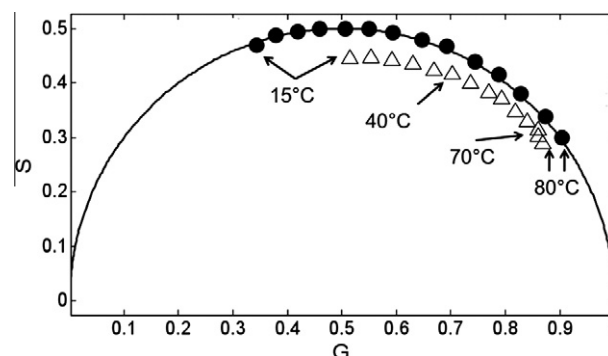
how temperature affects the phasor points for NATA and lysozyme. As shown in Fig. 3, the phasor points corresponding to NATA as a function of temperature remain on the universal circle and move clockwise as the temperature increases, indicating decreased lifetimes. The phasor points for lysozyme also progress clockwise with increasing temperatures, however, these points begin to migrate more toward the universal circle with increasing temperatures indicating decreases in the lifetime heterogeneity. This correlation of heterogeneity and temperature is similar to what was observed in human superoxide dismutase, which provided support for treatment of tryptophan decay as a continuous lifetime distribution [38]. At 70 °C, a change in trajectory occurs, likely indicating a complete thermal unfolding of the protein and a broadening of the distribution of lifetime values. These results are in agreement with the large volume of thermal denaturation literature on lysozyme [39,40]. Specifically, Morozova and coworkers [41], along with others, reported that the unfolding takes place in two steps, with the first reversible step occurring at approximately 40 °C and a second irreversible step occurring at approximately 70 °C.

Protein–ligand and protein–protein interactions

The sensitivity of tryptophan fluorescence to its environment makes it an ideal probe to monitor local and global structural movements and to provide insights into protein conformational changes associated with ligand binding. Using two protein systems, we investigated how phasor plots (derived from the intrinsic protein fluorescence) change during interactions with different ligands. Dynamin 2 is a 100-kDa GTPase associated with the pinching off of the plasma membrane during vesicle fission [42]. Dynamin 2 is composed of five domains—an N-terminal GTPase domain, a middle domain, a pleckstrin homology (PH) domain, a GTPase effector region (GED), and a proline/arginine-rich domain (PRD)—and contains five tryptophan residues, four of which are in the PH domain and one of which is in the C-terminal PRD. Previous work from our lab has shown that the tryptophans in dynamin can transfer energy to a fluorescent nucleotide [43,44]. In Fig. 4A, the phasor points of dynamin alone, GDP-bound dynamin, and GTPγS (a slowly hydrolyzable GTP analogue)-bound dynamin are presented. The data shown were collected with 300 nm excitation at 84 MHz and 20 °C. The addition of the guanine nucleotides clearly causes the phasor point to shift, and the position of the phasor point depends on the precise nucleotide used. These results indicate that there is a conformational change around one or more tryptophan residues associated with guanine nucleotide binding, moreover, the GDP and GTPγS ligands elicit different responses, indicating that the conformation of the protein matrix is not identical in the two cases. Solomaha and Palfrey [45], using steady state tryptophan fluorescence and limited proteolysis, concluded that

Fig.2. NATA (circles) and lysozyme (triangles) phasor points at 89 MHz, at 300 nm excitation and 20 °C, with the addition of various concentrations of acrylamide (0–0.2 M with NATA and 0–0.5 M with lysozyme).

Fig.3. Phasor plot, at 70 MHz and 280 nm excitation, of NATA (circles) and lysozyme (triangles) as a function of increasing temperatures.
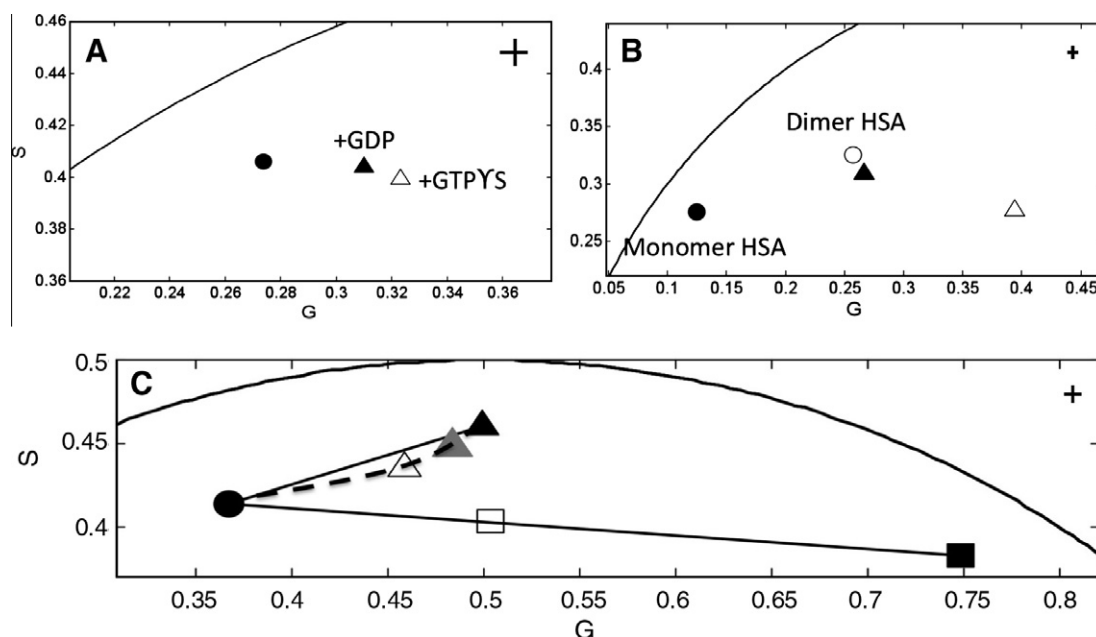
Fig.4. (A) Phasor plot for dynamin 2 alone (circle), GDP-bound dynamin (closed triangle), and GTPγS-bound dynamin (open triangle). (B) Monomeric HSA (closed circle) plotted with furosemide-bound HSA (open triangle) and D-thyroxine-bound HSA (closed triangle). Dimeric HSA (open circle), which can be found up to 10% in lyophilized HSA, has a unique decay/phasor point compared with monomeric HSA. (C) Phasor plot showing point movements due to protein–protein interaction. Solid lines between antithrombin (circle), lysozyme (closed square), and thrombin (closed triangle) are the projected linear movement of the phasor point for noninteracting species. Mixtures of antithrombin/lysozyme (both at 1 μM, open square) and antithrombin/thrombin (gray triangle 0.5:1;open triangle 1:1) are shown on the plot. The dashed line represents the projected phasor movement for increasing concentrations of antithrombin in the presence of thrombin. Crosshairs seen in the upper part of each figure represent the statistical error for each phasor point under the expanded phasor plot scale.

although GDP and GTP bind with similar affinities (13.0 and 7.1 μM, respectively), they produce distinct structural changes, in agreement with our phasor plot data.

HSA, which contains a single tryptophan residue (Trp214), has been the subject of numerous fluorescence studies, including time-resolved studies (see, e.g., [33,46–51]). HSA is commonly targeted for drug uptake studies, and often these drug interactions are studied via changes in tryptophan fluorescence. In Fig. 4B, we show the phasor point, collected using 300 nm excitation at 84 MHz and 25 °C, of the intrinsic fluorescence from monomeric HSA. In the presence of furosemide or D-thyroxine, two drugs known to bind to HSA and to quench the tryptophan fluorescence [11,52], the phasor point shifts clockwise, indicating a shortening of the average lifetime. These shifts in the phasor point indicate that drug binding induces changes in the protein matrix near the tryptophan residue and also that the conformational state of the protein differs depending on the nature of the drug, likely due to different binding sites (thyroxine has been shown to have multiple sites) on HSA. We also note that the phasor point corresponding to dimeric HSA, isolated from the monomeric protein using size exclusion chromatography, differs from the monomeric phasor point (seen in Fig. 4B). Hazan and coworkers [47] also showed that monomeric and dimeric HSA have different excited state lifetime properties. This difference underscores the necessity of isolating monomeric HSA from the aggregates usually found in commercial lyophilized preparations before undertaking a study of its intrinsic tryptophan fluorescence, an obvious step that, surprisingly, is sometimes overlooked.

One may also expect, from the previous sets of experiments, that protein–protein interactions could also be investigated using intrinsic tryptophan fluorescence and phasor plot analysis. For two interacting proteins with distinct average lifetimes, complex formation may be expected to change one or both protein conformations and result in a phasor point that deviates from the "normal" linear combination typically seen for noninteracting

mixtures [53]. Fig. 4C shows a set of data (acquired with 280 nm excitation at 43 MHz and 20 °C) for thrombin, antithrombin, lysozyme, and mixtures therein. Antithrombin and lysozyme are not predicted to interact, therefore a solution containing the two proteins should produce a phasor point that falls directly on a line between their individual points. This outcome is clearly observed (Fig. 4C) for the phasor plot of a 1:1 (at 1 μM) mixture of the two proteins. On the other hand, thrombin/antithrombin is known to form a tight complex [54] and may be expected to produce a distinct phasor point away from the linear combination. The phasor point of the thrombin/antithrombin (1:1 at 1 μM for each protein) indeed shifts inward away from the line connecting the points corresponding to the two pure proteins, indicating a change in intrinsic fluorescence on protein interaction. This demonstration shows how phasor plots can provide a facile indication of protein interaction.

Kinetics of protein–ligand binding/dissociation

Determination of the rate constants associated with protein–ligand binding/dissociation reactions is a major goal in many studies. Kinetics of such reactions often proceed on a rapid time scale (seconds to a few minutes). Steady state fluorescence methodologies, such as stopped-flow fluorescence, are frequently preferred over lifetime methods because traditional frequency domain lifetime measurements usually require 1 or 2 min for reasonable precision (although specialized fast scanning methods are available) [55,56]. However, the phasor plot method, recorded at a single frequency, is well-suited for rapidly tracking changes in the phase and modulation data. To illustrate this point and validate the phasor method for tracking kinetics of protein–ligand dissociation, the phase and modulation of the intrinsic fluorescence of human serum transferrin (the isolated N-lobe) were recorded over approximately 300 s at 80 MHz in pH 6.0 buffer and the presence of a chelator. Human serum transferrin (hTF) is a bilobal glycoprotein

that serves as the major transporter of iron in humans (reviewed in [57]). Both lobes, termed the N- and C-lobes, coordinate ferric iron via four amino acid ligands and a synergistic carbonate anion. Numerous studies on hTF have shown that binding of iron quenches the intrinsic tryptophan fluorescence through radiative and nonradiative means [14,58,59]. Thus, rate constants for iron removal are determined by tracking the enhancement in fluorescence emission over time under endosomal-like conditions (∼pH 5.5, ∼150–200 mM salt, and the presence of a chelator), and this takes place within seconds to minutes.

The lifetime of iron-bound and apo hTF N-lobe (which contains three tryptophan residues) was determined previously [58]. The two discrete lifetime values associated with the hTF N-lobe (∼1.4 and ∼4.1 ns) undergo minimal change (±0.3 ns) during iron removal. The fractional fluorescence of each lifetime component, however, undergoes large changes (0.66/0.28 for iron-bound and 0.20/0.79 for apo). Based on the theoretical description (see previous article), the decay during iron release would be predicted to be a line between the iron-bound and apo phasor points. Fig. 5, which shows the phasor plot (taken at 80 MHz and 300 nm excitation) during iron release (black line) and the points for iron-bound (circle) and apo (triangle), clearly demonstrates the predicted linear progression in the phasor point during iron release from the iron-bound point toward the apo phasor point. Sample heterogeneity, which was expected based on the fitting to a discrete exponential model, is seen in the phasor vectors of hTF N-lobe given that each point is inside the universal circle. Calculation of the distance at each point over time can provide information regarding excited state changes during iron removal (i.e., one can recover the fractional contribution of each emitting state using standard linear methods). Interestingly, the phasor data during iron release indicate that the change in the excited state properties of the hTF N-lobe occurs in two modes: a faster initial mode (during the first ∼90 s) followed by a slower progression toward apo (∼90–300 s). These results are similar to those observed following the steady state emission changes, in which the faster rate was conclusively determined to be iron release and the slower rate was assigned to conformational events [14]. Data can be acquired on a subsecond time scale with the use of a stopped-flow attachment, however, such an attachment was not available to us to directly demonstrate more rapid measurements. This kinetic run demonstrates how the phasor method can be used for tracking excited state changes during protein–ligand dissociation, which can complement data obtained using other methods. We also point out that the phasor approach was applied in fluorescence lifetime imaging

(FLIM) by Redford and Clegg [53] to follow the kinetics of mixing in turbulent flow at the microsecond time scale.

Protein unfolding/folding pathways

Protein folding has been intensely investigated, both theoretically and experimentally, for many decades. One of the most popular experimental approaches to protein folding involves examination of the unfolding pathway(s) by means of chemical denaturation [60,61]. Chaotropic agents, such as GdHCl and urea, are commonly used denaturants. Unfolding experiments using such chemical denaturants have one major underlying assumption—that the overall thermodynamic unfolding of the protein is independent of denaturing agent, although the structural changes associated with the change are dependent [62,63]. The molecular mechanisms for protein unfolding by GdHCl and urea are still unclear, even though mechanisms were proposed as early as 1936 [64]. Models describing the direct interaction of the denaturant with the protein and disruption of the hydrophobic interactions via disruption of the hydrogen bonding network are the commonly accepted mechanisms [65,66]. Recently, Almarza and coworkers [67] proposed a more detailed model for urea-induced protein unfolding in which urea molecules interact with protonated histidines followed by hydrogen bond formation with polar residues, leading to hydrophobic collapse of the protein.

Because the detailed molecular mechanisms for protein unfolding due to GdHCl and urea are likely different, it would stand to reason that the intrinsic fluorescence properties will be different during denaturation depending on which chaotropic agent is present. Tryptophan fluorescence is sensitive to changes in the local environment, and if the structural changes leading to unfolding of the protein are intrinsically different, then the environment around the tryptophan residues could differ depending on the chaotropic agent, resulting in distinct fluorescence properties. The phasor plot of lysozyme with increasing concentrations of GdHCl (0–6 M) and urea (0–8 M) is shown in Fig. 6. Initial additions of either denaturant cause similar changes, yet by 2 M the trajectories of the phasor points diverge, with GdHCl shifting the phasor points in a counterclockwise direction. The final points between GdHCl and urea are dramatically different, indicating unique unfolded forms. Similar deviations between unfolding with GdHCl and urea were observed with monomeric HSA (data not shown). It is clear that the phasor plot method has the potential for illustrating different unfolding pathways given that both proteins tested showed significant deviations in phasor point trajectories depending on the denaturant.
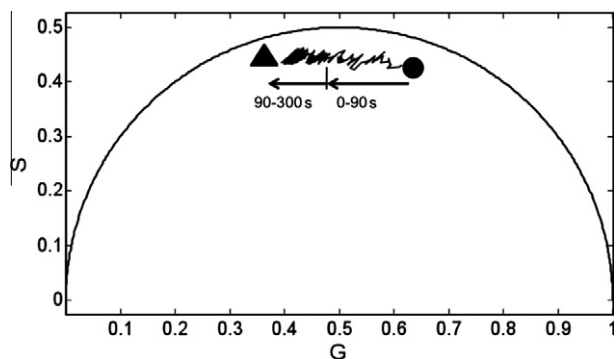
Fig.5. Phasor plot of iron release from hTF N-lobe. Iron-bound and apo phasor vectors are drawn as circle and triangle, respectively. The change in phasor during iron removal, at pH 6.0 with 4 mM ethylenediaminetetraacetic acid (EDTA) over 300 s, is drawn as a black line. Over the first ∼ 90 s, there is a rapid change in the excited state data followed by a much slower change. Data shown were collected at 80 MHz and 25 °C.
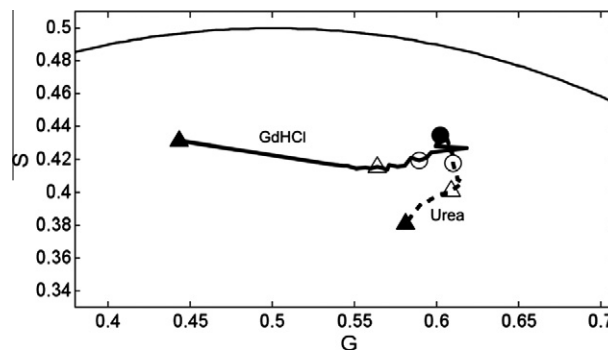
Fig.6. Phasor point trajectory of lysozyme denaturation as a function of increasing GdHCl (solid line) and urea (dashed line) concentrations. Concentrations of 0 M (closed circle), 1 M (open circle), 2 M (open triangle), and 6/8 M (closed triangle) GdHCl and urea are highlighted. Data were recorded at 280 nm, and data plotted were at 70 MHz and 25 °C.

Conclusions

In this article, we have described the application of the phasor method to time-resolved studies on intrinsic protein fluorescence. Using this approach, the complex decay of protein fluorescence, due to either multiple emitting tryptophan residues or excited state reactions such as tyrosine-to-tryptophan energy transfer, can be reduced to a single point on a phasor plot. Activities such as ligand or protein binding and protein denaturation, which result in changes in the microenvironment of the tryptophan residue(s), lead to movements of the phasor point. The trajectory of the phasor point in response to a physical or chemical perturbation can be followed to provide insights into the processes under investigation.

Acknowledgments

References

[1] B. Valeur, Molecular Fluorescence, Wiley–VCH, Weiheim;Germany, 2002.
[2] J.A. Ross, D.M. Jameson, Time-resolved methods in biophysics: 8. Frequency domain fluorometry – applications to intrinsic protein fluorescence, Photochem. Photobiol. Sci. 7 (2008) 1301–1312.
[3] G. Weber, Resolution of the fluorescence lifetimes in a heterogeneous system by phase and modulation measurements, J. Phys. Chem. 85 (1981) 949–953.
[4] J.R. Alcala, E. Gratton, F.G. Prendergast, Interpretation of fluorescence decays in proteins using continuous lifetime distributions, Biophys. J. 51 (1987) 925–936.
[5] J.C. Brochon, Maximum entropy method of data analysis in time-resolved spectroscopy, Methods Enzymol. 240 (1994) 262–311.
[6] J.M. Beecham, L. Brand, Time-resolved fluorescence of proteins, Annu. Rev. Biochem. 54 (1985) 43–71.
[7] C.N. Bialik, B. Wolf, E.L. Rachofsky, J.B. Ross, W.R. Laws, Dynamics of biomolecules: assignment of local motions by fluorescence anisotropy decay, Biophys. J. 75 (1998) 2564–2573.
[8] J.T. Vivian, P.R. Callis, Mechanisms of tryptophan fluorescence shifts in proteins, Biophys. J. 80 (2001) 2093–2109.
[9] J.B. Ross, A.G. Szabo, C.W. Hogue, Enhancement of protein spectra with tryptophan analogs: fluorescence spectroscopy of protein–protein and protein–nucleic acid interactions, Methods Enzymol. 278 (1997) 151–190.
[10] N.G. James, S.L. Byrne, A.B. Mason, Incorporation of 5-hydroxytryptophan into transferrin and its receptor allows assignment of the pH induced changes in intrinsic fluorescence when iron is released, Biochim. Biophys. Acta 1794 (2009) 532–540.
[11] J.R. Voelker, D.M. Jameson, D.C. Brater, In vitro evidence that urine composition affects the fraction of active furosemide in the nephrotic syndrome, J. Pharmacol. Exp. Ther. 250 (1989) 772–778.
[12] Z. Akyol, J.A. Bartos, M.A. Merrill, L.A. Faga, O.R. Jaren, M.A. Shea, J.W. Hell, Apo-calmodulin binds with its C-terminal domain to the N-methyl-D-aspartate receptor NR1 C0 region, J. Biol. Chem. 279 (2004) 2166–2175.
[13] C.A. Dunlap, M.D. Tsai, Use of 2-aminopurine and tryptophan fluorescence as probes in kinetic analyses of DNA polymerase beta, Biochemistry 41 (2002) 11226–11235.
[14] N.G. James, C.L. Berger, S.L. Byrne, V.C. Smith, R.T. MacGillivray, A.B. Mason, Intrinsic fluorescence reports a global conformational change in the N-lobe of human serum transferrin following iron release, Biochemistry 46 (2007) 10603–10611.
[15] D.M. Jameson, E. Gratton, J.F. Eccleston, Intrinsic fluorescence of elongation factor Tu in its complexes with GDP and elongation factor Ts, Biochemistry 26 (1987) 3894–3901.
[16] V.V. Bulygin, Y.M. Milgrom, Studies of nucleotide binding to the catalytic sites of Escherichia coli βY331W–F1-ATPase using fluorescence quenching, Proc. Natl. Acad. Sci. USA 104 (2007) 4327–4331.
[17] S.S. Lehrer, Solute perturbation of protein fluorescence. The quenching of the tryptophyl fluorescence of model compounds and of lysozyme by iodide ion, Biochemistry 10 (1971) 3254–3263.
[18] M.R. Eftink, C.A. Ghiron, Dynamics of a protein matrix revealed by fluorescence quenching, Proc. Natl. Acad. Sci. USA 72 (1975) 3290–3294.
[19] J.R. Lakowicz, G. Weber, Quenching of fluorescence by oxygen: a probe for structural fluctuations in macromolecules, Biochemistry 12 (1973) 4161–4170.
[20] J.R. Unruh, K. Kuczera, C.K. Johnson, Conformational heterogeneity of a leucine enkephalin analogue in aqueous solution and sodium dodecyl sulfate micelles: comparison of time-resolved FRET and molecular dynamics simulations, J. Phys. Chem. B 113 (2009) 14381–14392.
[21] D.M. Rayner, A.G. Szabo, Time resolved fluorescence of aqueous tryptophan, Can. J. Chem. 56 (1978) 743–745.
[22] P.R. Callis, ^1L_a and ^1L_b transitions of tryptophan: applications of theory and experimental observations to fluorescence of proteins, Methods Enzymol. 278 (1997) 113–150.
[23] A.H. Clayton, W.H. Sawyer, Tryptophan rotamer distributions in amphipathic peptides at a lipid surface, Biophys. J. 76 (1999) 3235–3242.
[24] Y. Chen, M.D. Barkley, Toward understanding tryptophan fluorescence in proteins, Biochemistry 37 (1998) 9976–9982.
[25] N.G. James, M. Stefl, J.A. Ross, D.M. Jameson, Application of phasor plots to analysis of fluorophore heterogeneity;excited state reactions;and protein conformations, Biophys. J. 98 (2010) 750a.
[26] H.R. Costantino, L. Shieh, A.M. Klibanov, R. Langer, Heterogeneity of serum albumin samples with respect to solid-state aggregation via thiol–disulfide interchange: implications for sustained release from polymers, J. Control. Release 44 (1997) 255–261.
[27] C.N. Pace, F. Vajdos, L. Fee, G. Grimsley, T. Gray, How to measure and predict the molar absorption coefficient of a protein, Protein Sci. 4 (1995) 2411–2423.
[28] B. Barbieri, E. Terpetschnig, D.M. Jameson, Frequency-domain fluorescence spectroscopy using 280-nm and 300-nm light-emitting diodes: measurement of proteins and protein-related fluorophores, Anal. Biochem. 344 (2005) 298–300.
[29] R.D. Spencer, G. Weber, Influence of Brownian rotations and energy transfer upon the measurements of fluorescence lifetime, J. Chem. Phys. 52 (1970) 1654–1663.
[30] N. Boens, W. Qin, N. Basaric, J. Hofkens, M. Ameloot, J. Pouget, J.P. Lefevre, B. Valeur, E. Gratton, M. Van De Ven, N.D. Silva Jr., Y. Engelborghs, K. Willaert, A. Sillen, G. Rumbles, D. Phillips, A.J. Visser, A. van Hoek, J.R. Lakowicz, H. Malak, I. Gryczynski, A.G. Szabo, D.T. Krajcarski, N. Tamai, A. Miura, Fluorescence lifetime standards for time and frequency domain fluorescence spectroscopy, Anal. Chem. 79 (2007) 2137–2149.
[31] M. Stefl, N.G. James, J.A. Ross, D.M. Jameson, Applications of phasors to in vitro time-resolved fluorescence measurements, Anal. Biochem. (2010), doi:10.1016/j.ab.2010.11.010.
[32] A. White, Effect of pH on fluorescence of tryosine, tryptophan, and related compounds, Biochem. J. 71 (1959) 217–220.
[33] W.B. De Lauder, P. Wahl, PH dependence of the fluorescence decay of tryptophan, Biochemistry 9 (1970) 2750–2754.
[34] D.M. Jameson, G. Weber, Resolution of the pH-dependent heterogeneous fluorescence decay of tryptophan by phase and modulation measurements, J. Phys. Chem. 85 (1981) 953–958.
[35] R.D. Spencer, G. Weber, Measurement of subnanosecond fluorescence lifetimes with a cross-correlation phase fluorometer, Annu. NY Acad. Sci. 158 (1969) 361–376.
[36] T. Imoto, L.S. Forster, J.A. Rupley, F. Tanaka, Fluorescence of lysozyme: emissions from tryptophan residues 62 and 108 and energy migration, Proc. Natl. Acad. Sci. USA 69 (1972) 1151–1155.
[37] S.S. Lehrer, G.D. Fasman, Fluorescence of lysozyme and lysozyme substrate complexes: separation of tryptophan contributions by fluorescence difference methods, J. Biol. Chem. 242 (1967) 4644–4651.
[38] N. Rosato, E. Gratton, G. Mei, A. Finazzi-Agro, Fluorescence lifetime distributions in human superoxide dismutase. Effect of temperature and denaturation, Biophys. J. 58 (1990) 817–822.
[39] S. Segawa, M. Nakayama, M. Sakane, Rates of structural fluctuations of lysozyme in the range of thermal unfolding transition, Biopolymers 20 (1981) 1691–1705.
[40] J. Jacob, C. Krafft, K. Welfle, H. Welfle, W. Saenger, Melting points of lysozyme and ribonuclease A crystals correlated with protein unfolding: a Raman spectroscopic study, Acta Crystallogr. D 54 (1998) 74–80.
[41] L. Morozova, P. Haezebrouck, F. Van Cauwelaert, Stability of equine lysozyme: I. Thermal unfolding behaviour, Biophys. Chem. 41 (1991) 185–191.
[42] S.D. Conner, S.L. Schmid, Regulated portals of entry into the cell, Nature 422 (2003) 37–44.
[43] D.D. Binns, M.K. Helms, B. Barylko, C.T. Davis, D.M. Jameson, J.P. Albanesi, J.F. Eccleston, The mechanism of GTP hydrolysis by dynamin II: a transient kinetic study, Biochemistry 39 (2000) 7188–7196.
[44] J.F. Eccleston, D.D. Binns, C.T. Davis, J.P. Albanesi, D.M. Jameson, Oligomerization and kinetic mechanism of the dynamin GTPase, Eur. Biophys. J. 31 (2002) 275–282.
[45] E. Solomaha, H.C. Palfrey, Conformational changes in dynamin on GTP binding and oligomerization reported by intrinsic and extrinsic fluorescence, Biochem. J. 391 (2005) 601–611.
[46] S. Kasai, T. Horie, T. Mizuma, S. Awazu, Fluorescence energy transfer study of the relationship between the lone tryptophan residue and drug binding sites in human serum albumin, J. Pharm. Sci. 76 (1987) 387–392.
[47] G. Hazan, E. Haas, I.Z. Steinberg, The fluorescence decay of human serum albumin and its subfractions, Biochim. Biophys. Acta 434 (1976) 144–153.
[48] P. Marzola, E. Gratton, Hydration and protein dynamics: frequency domain fluorescence spectroscopy of proteins in reverse micelles, J. Phys. Chem. 95 (1991) 9488–9495.
[49] J.R. Lakowicz, I. Gryczynski, Tryptophan fluorescence intensity and anisotropy decays of human serum albumin resulting from one-photon and two-photon excitation, Biophys. Chem. 45 (1992) 1–6.

[50] D.M. Davis, D. McLoskey, D.J. Birch, P.R. Gellert, R.S. Kittlety, R.M. Swart, The fluorescence and circular dichroism of proteins in reverse micelles: application to the photophysics of human serum albumin and *N*-acetyl-L-tryptophanamide, Biophys. Chem. 60 (1996) 63–77.

[51] M.K. Helms, C.E. Petersen, N.V. Bhagavan, D.M. Jameson, Time-resolved fluorescence studies on site-directed mutants of human serum albumin, FEBS Lett. 408 (1997) 67–70.

[52] C.E. Petersen, C.E. Ha, D.M. Jameson, N.V. Bhagavan, Mutations in a specific human serum albumin thyroxine binding site define the structural basis of familial dysalbuminemic hyperthyroxinemia, J. Biol. Chem. 271 (1996) 19110–19117.

[53] G.I. Redford, R.M. Clegg, Polar plot for frequency-domain analysis of fluorescence lifetimes, J. Fluoresc. 15 (2005) 805–815.

[54] D. Beeler, R. Rosenberg, R. Jordan, Fractionation of low molecular weight heparin species and their interaction with antithrombin, J. Biol. Chem. 254 (1979) 2902–2913.

[55] O. Bilsel, L. Yang, J.A. Zitzewitz, J.M. Beechem, C.R. Matthews, Time-resolved fluorescence anisotropy study of the refolding reaction of the α-subunit of tryptophan synthase reveals nonmonotonic behavior of the rotational correlation time, Biochemistry 38 (1999) 4177–4187.

[56] B.A. Feddersen, D.W. Piston, E. Gratton, Digital parallel acquisition in frequency domain fluorimetry, Rev. Sci. Instrum. 60 (1989) 2929–2936.

[57] A.B. Mason, S.J. Everse, Iron transport by transferrin, in: H. Fuchs (Ed.), Iron Metabolism and Disease, Research Signpost, Kerala, India, 2008, pp. 83–123.

[58] N.G. James, J.A. Ross, A.B. Mason, D.M. Jameson, Excited-state lifetime studies of the three tryptophan residues in the N-lobe of human serumn transferrin, Protein Sci. (2010) 99–110.

[59] S.S. Lehrer, Fluorescence and absorption studies of the binding of copper and iron to transferrin, J. Biol. Chem. 244 (1969) 3613–3617.

[60] K.A. Dill, S.B. Ozkan, M.S. Shell, T.R. Weikl, The protein folding problem, Annu. Rev. Biophys. 37 (2008) 289–316.

[61] A.R. Fersht, From the first protein structures to our current knowledge of protein folding: delights and scepticisms, Nat. Rev. Mol. Cell Biol. 9 (2008) 650–654.

[62] W. Pfeil, P.L. Privalov, Thermodynamic investigations of proteins: II. Calorimetric study of lysozyme denaturation by guanidine hydrochloride, Biophys. Chem. 4 (1976) 33–40.

[63] G.I. Makhatadze, P.L. Privalov, Protein interactions with urea and guanidinium chloride: a calorimetric study, J. Mol. Biol. 226 (1992) 491–505.

[64] A.E. Mirsky, L. Pauling, On the structure of native;denatured;and coagulated proteins, Proc. Natl. Acad. Sci. USA 22 (1936) 439–447.

[65] R.B. Simpson, W. Kauzmann, The kinetics of protein denaturation: I. The behavior of the optical rotation of ovalbumin in urea solutions, J. Am. Chem. Soc. 75 (1953) 5139–5152.

[66] M. Roseman, W.P. Jencks, Interactions of urea and other polar compounds in water, J. Am. Chem. Soc. 97 (1975) 631–640.

[67] J. Almarza, L. Rincon, A. Bahsas, F. Brito, Molecular mechanism for the denaturation of proteins by urea, Biochemistry 48 (2009) 7608–7613.